

CHAPTER 128

HEAD LOSS AT TSUNAMI-BREAKWATER OPENING

by Yoshiyuki ITO*

Abstract

The head loss at breakwater opening is an important factor for evaluating the effect of breakwaters against tsunami. This paper examines the coefficient of the head loss term in the equation of motion by comparing the results of numerical calculations with the actual record observed in the Port of Ofunato at the time of 1968 tsunami. Numerical calculations are repeated changing the head loss coefficient from zero to 3.0 with the interval of 0.5. The calculated water level variation is quite different from the record if no head loss is taken into consideration. Although the most suitable value of the coefficient is not definitely determined, the value of 1.5, which has been adopted in our previous calculations, seems to be reasonable for practical purpose.

Introduction

The construction of tsunami-breakwaters in the Port of Ofunato and several other harbours was started after the disaster due to Chilean Earthquake Tsunami in 1960. Concerning this project the author studied the effect of breakwaters against tsunami mainly by numerical calculations. The method of calculation and some results obtained were reported to 10th Coastal Engineering Conference held in Tokyo in 1966 (Reference 1).

In May 1968, the tsunami-breakwater in the Port of Ofunato experienced the first remarkable tsunami since its completion in 1967. The water level variation was recorded by two tide gauges located outside and inside the breakwater. The author immediately applied the method of calculation and obtained a good agreement between calculation and observation. The effect of the tsunami-breakwater was also confirmed by this analysis. The details were already reported to 13th IAHR Congress in Kyoto, 1969 (Reference 2).

The term of head loss included in the equation of motion at the breakwater opening plays an important role in numerical calculation. If no head loss is taken into account, the effect of breakwaters against tsunami is not appropriately evaluated due to the appearance of so-called harbor-paradox. The author has so far adopted the head loss coefficient of 1.5 in previous calculations. The influence of this coefficient on the calculated results is examined in this paper by comparing the calculations with the actual observation of 1968 tsunami in the Port of Ofunato.

* Hydraulics Division, Port and Harbour Research Institute, Ministry of Transport 3-1-1, Nagase, Yokosuka, Japan

Basic Equations

The principle of calculation is to solve numerically the equations of motion and of continuity for two-dimensional long wave under certain initial and boundary conditions. Fundamental equations are as follows,

$$\begin{aligned}\frac{\partial u}{\partial t} &= -g \frac{\partial \zeta}{\partial x} \\ \frac{\partial v}{\partial t} &= -g \frac{\partial \zeta}{\partial y} \\ \frac{\partial \zeta}{\partial t} &= -\frac{\partial}{\partial x} (hu) - \frac{\partial}{\partial y} (hv)\end{aligned}\quad (1)$$

where, u, v = velocity component in x - and y -direction, respectively
 ζ = water level elevation with respect to mean water level
 h = water depth below mean water level

These differential equations are transformed into difference equations. Figure 1 shows the grid system around the breakwater in the Port of Ofunato. The grid interval in this case is 280 metres and the time interval is 10 seconds.

The outer sea is replaced by a channel of constant depth and width, where the computation is only aimed at supplying the incoming tsunami without being affected by reflected waves from the breakwater and shorelines. As a boundary condition, velocity components normal to the breakwater and shorelines are given to be zero. The calculation is started from the time when the front of tsunami arrives at the bay-mouth. Initial water level and velocity inside the bay are accordingly zero, while those in the outer sea correspond to the incident tsunami profile.

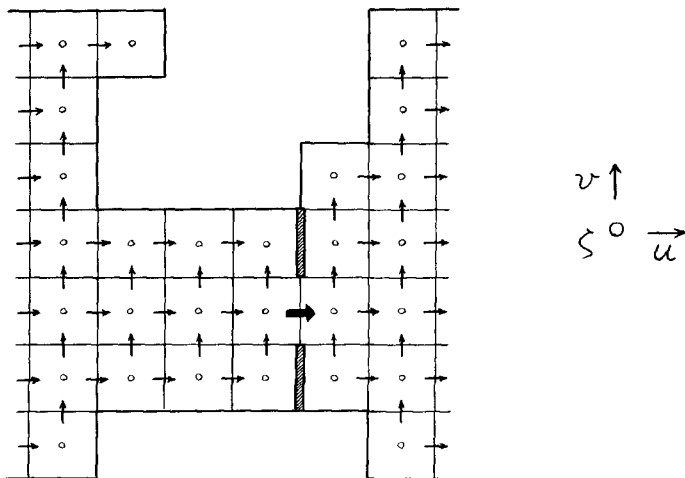


Figure 1 Grid System for Numerical Calculation

Although higher order terms for inertia or bottom friction are neglected in Equation (1), a term representing the head loss is added to the equation of motion at the breakwater opening as shown in the following difference equation,

$$\frac{\Delta u}{\Delta t} = -g \frac{\Delta \eta}{\Delta x} - \frac{f}{2\Delta x} - u|u| \quad (2)$$

The head loss coefficient f in this equation has been assumed to be 1.5 in previous calculations. In this paper numerical calculations are carried out with f of 0, 0.5, 1.0, .., 3.0.

1968 tsunami in the Port of Ofunato

Figure 2 shows the plan of Ofunato Bay situated in the north-eastern part of Japan along the Pacific Coast. The tsunami-breakwater near the bay-mouth, where the maximum water depth reaches almost 40 metres, was constructed after Chilean Earthquake Tsunami in 1960 and was completed in 1967.

On May 16, 1968, an earthquake of magnitude 7.8 occurred off this district. A tsunami accompanied by this earthquake attacked the coast and caused certain damages to several ports. The tsunami-breakwater in the Port of Ofunato effectively protected the harbour and the city by reducing the water level elevation in the inner basin.

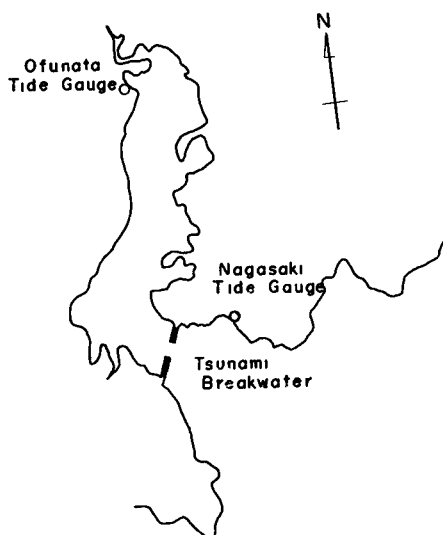


Figure 2 Tsunami-breakwater and Tide Gauges in the Port of Ofunato

Actual records of water level variation were obtained at two tide gauges, the one is located between the bay-mouth and the breakwater (Nagasaki) and the other is at the innermost part of the bay (Ofunato). The position of these tide gauges is indicated in Figure 2.

Figure 3 shows the water level variations during the first two hours, the astronomical tide being subtracted.

In the analysis of this tsunami by applying the author's method, the incident tsunami profile for calculation was determined so that the calculated water level variation at the outside tide gauge might be as close as possible to the observation. The outline of the procedure for this determination is as the following,

1) The water level variation at the outside tide gauge during the first 124 minutes, in which most of the major fluctuations are included, is analyzed into Fourier sine series.

2) Calculations are repeated for component regular sinusoidal waves in order to obtain the amplifying factor at the outside tide gauge. The amplifying factor obtained varies from 1.7 to 2.9.

3) The amplitude of each component obtained in the item 1) is divided by the corresponding amplifying factor in the item 2). The Fourier sine series consisting of thus determined amplitudes gives the approximate profile of the incident tsunami.

With this incident tsunami profile, a good agreement was confirmed between the calculation and the observation at the inside tide gauge. A calculation with the same incident tsunami was also carried out for the harbour before the construction of the tsunami-breakwater. The highest water level elevation in the harbour after the breakwater construction is 1.1-1.2 metres, while without the breakwater it reaches more than 2 metres. The effect of the tsunami-breakwater is definitely evaluated by these numerical calculations

Influence of the head loss coefficient on calculated results

The incident tsunami profile determined by the above-mentioned procedure will be affected to a certain extent by the head loss coefficient at the breakwater opening. However, the profile for $f=1.5$ is commonly used in this paper to all the cases from $f=0$ to 3.0. The influence of the value of f on the water level at the outside tide gauge is comparatively small, as shown in Figure 4.

Figure 5 is the comparison between calculation and observation at the inside tide gauge. This figure indicates that the curve for $f=0$ is quite different from the actual record, not only in the value at each peak or trough but also in the form of the curve itself.

Table 1 shows the computed and observed water level elevations at several peaks and troughs. The value of f fitted to the observation differs at each position, as indicated by the mark (*) in the column of calculation.

Figure 6 shows the goodness of fit of computed water level. The goodness is measured by the root mean square (σ) of the residuals at every two minutes during two hours ($N=60$).

$$\sigma = \sqrt{\sum (\xi_{\text{cal}} - \xi_{\text{obs}})^2 / N} \quad (3)$$

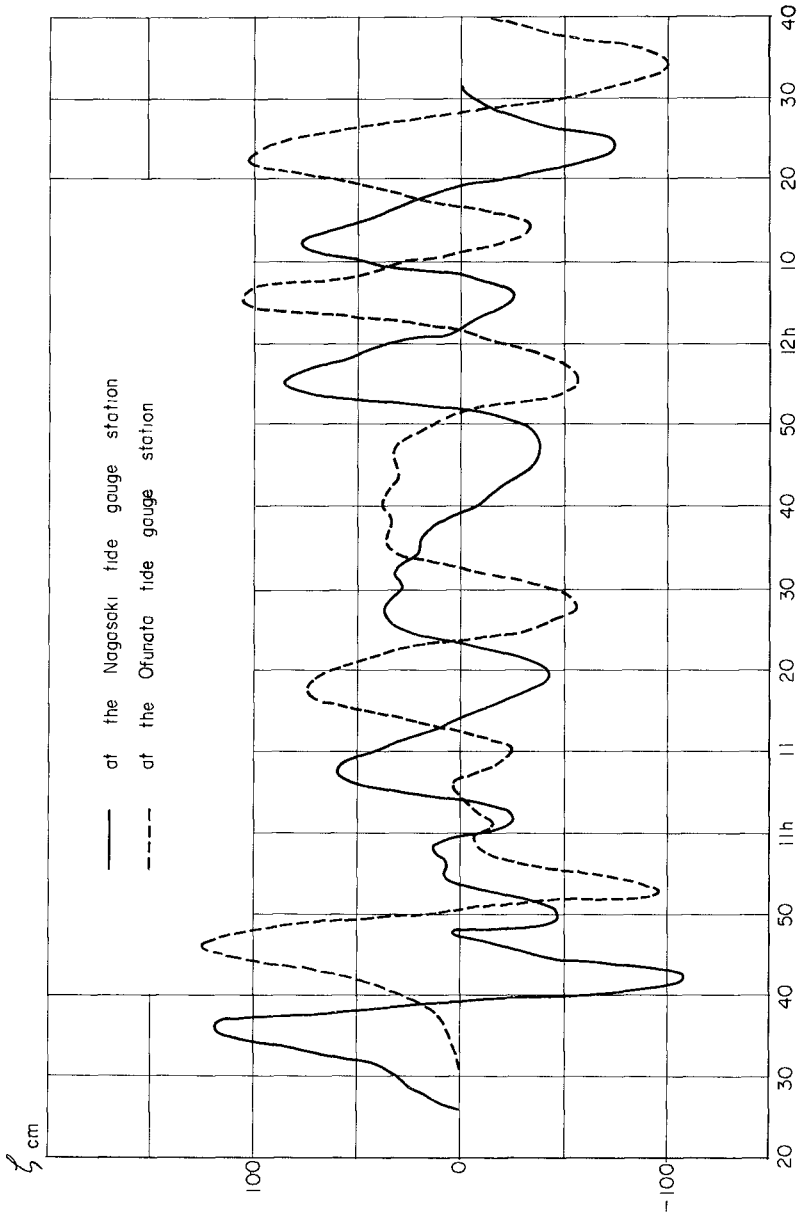


Figure 3 Water Level Variation due to 1968 Tsunami in the Port of Ofunata

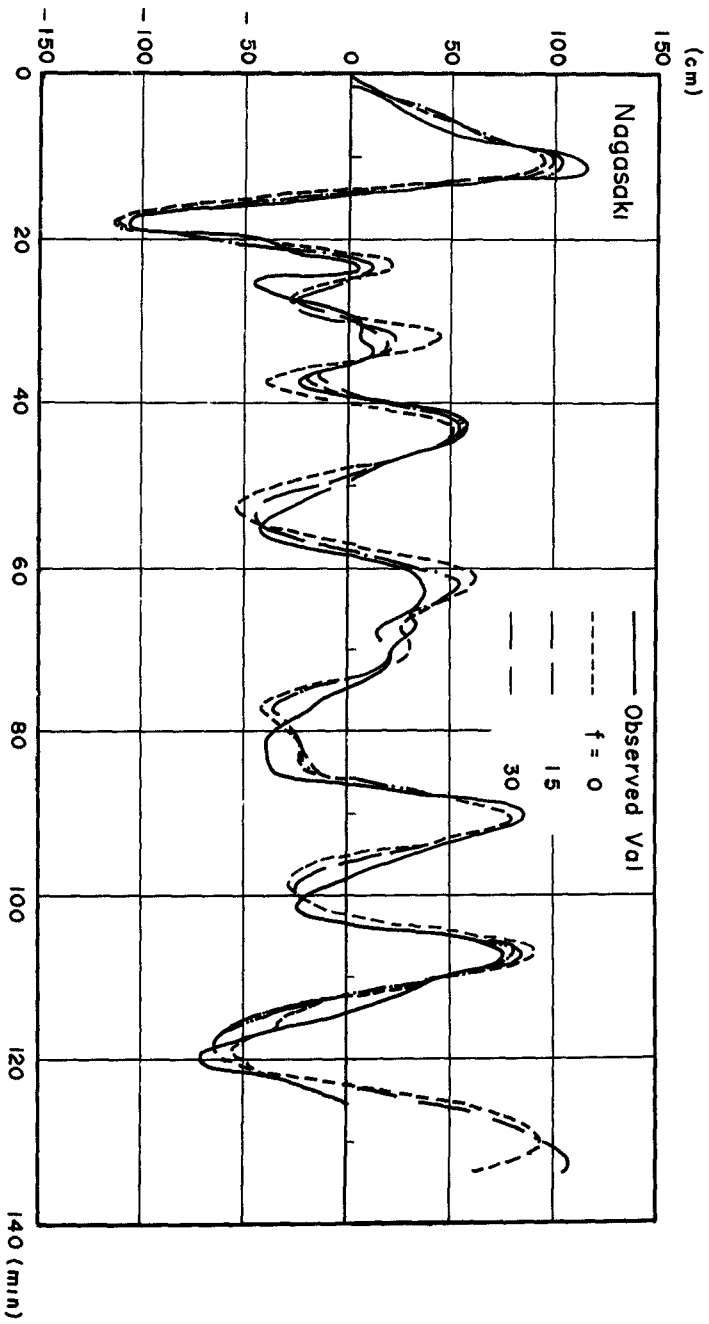


Figure 4 Comparison of Calculation and Observation at the Outside Tide Gauge

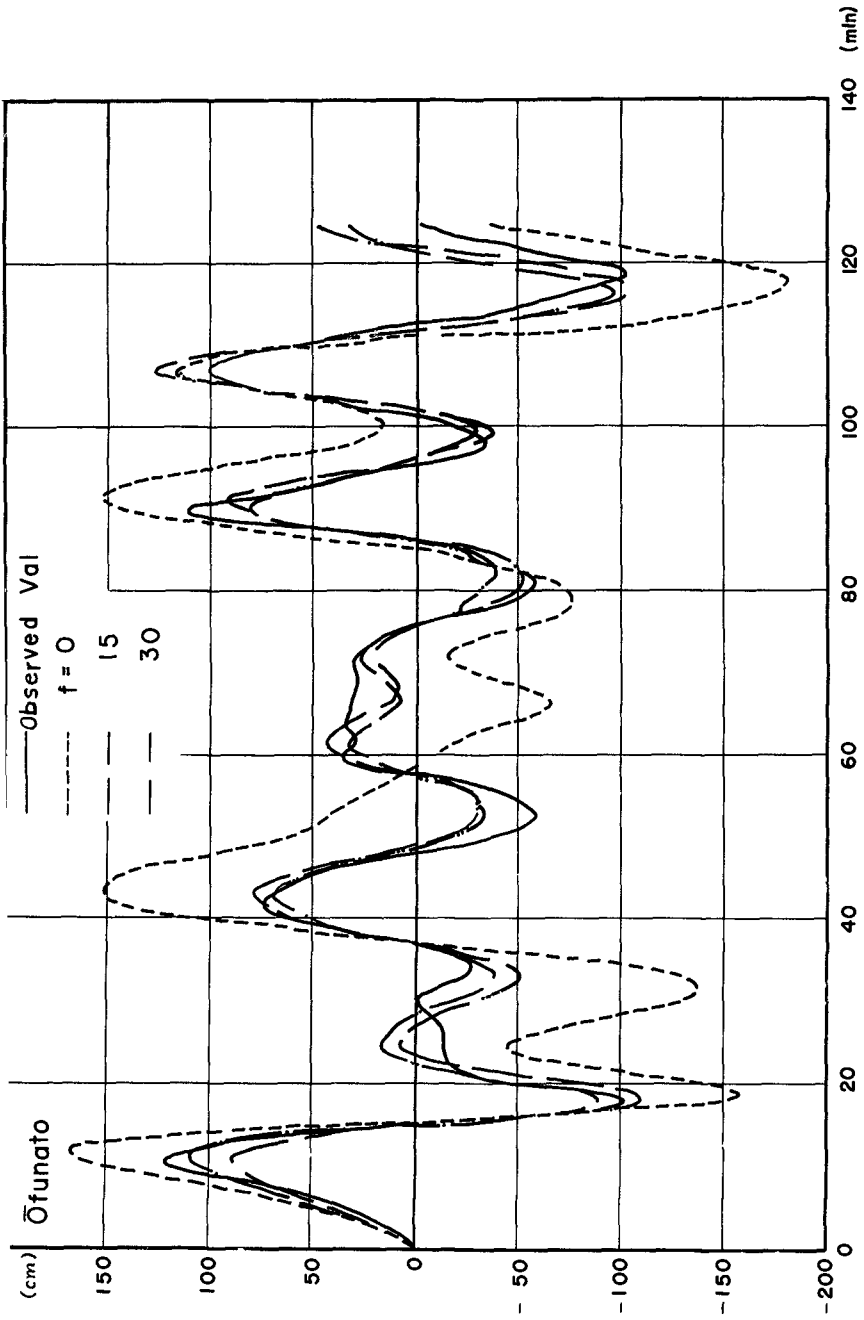


Figure 5 Comparison of Calculation and Observation at the Inside Tide Gauge

Table 1 Comparison of Calculation and Observation
at Peaks and Troughs (unit cm)

Position	Observation	Calculation						
		f=0	0.5	1.0	1.5	2.0	2.5	3.0
1st peak	124	169	140	123*	111	103	96	91
1st trough	-102	-159	-137	-120	-108	-101*	-95	-90
3rd peak	74	153	104	88	80	75*	72	69
4th peak	112	153	108*	100	94	90	85	81
6th peak	102	119	138	134	129	123	119	115*
6th trough	-101	-180	-121	-111	-105	-102*	-99	-97

Although the incident tsunami profile has been determined so that the computed water level at the outside tide gauge might coincide with the observed record, there still remain some differences between calculation and observation. The deviation of calculation for the inside tide gauge will depend on both the accuracy of the incident tsunami profile and the value of the head loss coefficient f .

At the inside tide gauge, the root mean square of the residuals is very big at $f=0$. It decreases rapidly with the increase of f and becomes almost constant for f of bigger than 1.0.

It is not easy to find out definitely the most suitable value of f from these results. However, the analysis in this paper suggests the practical validity of the adoption of 1.5 or so as the head loss coefficient at the tsunami-breakwater opening, as far as the form of the equation of motion in our method of calculation is concerned.

References

- 1) H. Fukuuchi, Y. Ito On the Effect of Breakwaters against Tsunami, Proc. 10th Conference on Coastal Engineering (Tokyo, 1966), pp.821-839
- 2) Y. Ito On the Effect of Ofunato Tsunami-Breakwater against 1968 Tsunami, Proc. 13th Congress of IAHR (Kyoto, 1969), Vol.3, pp.85-93

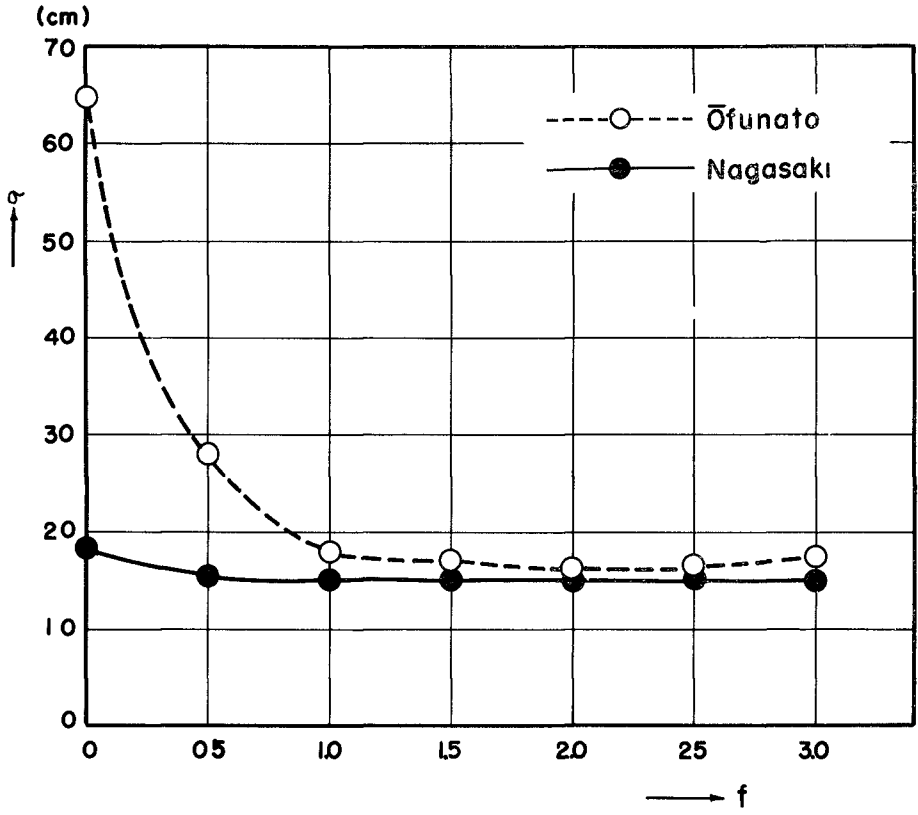


Figure 6 Goodness of Fit

